Toxicology Letters 301 (2019) 53–63

Contents lists available at ScienceDirect

Toxicology Letters

journal homepage: www.elsevier.com/locate/toxlet

Involvement of NLRP3 inflammasome in methamphetamine-induced microglial activation through miR-143/PUMA axis

Longfei Du[a], Kai Shen[b], Ying Bai[a], Jie Chao[c], Gang Hu[d], Yuan Zhang[a,*], Honghong Yao[a,e,*]

[a] Department of Pharmacology, School of Medicine, Southeast University, Nanjing, Jiangsu, China
[b] Department of Pharmacology, Affiliated Hospital of Nantong University, Nantong, Jiangsu, China
[c] Department of Physiology, School of Medicine, Southeast University, Nanjing, Jiangsu, China
[d] Jiangsu Key Laboratory of Neurodegeneration, Department of Pharmacology, Nanjing Medical University, Nanjing, 210029, Jiangsu, China
[e] Institute of Life Sciences, Key Laboratory of Developmental Genes and Human Disease, Southeast University, Nanjing, 210096, Jiangsu, China

ARTICLE INFO

Keywords:
NLRP3
miR-143
PUMA
Methamphetamine
Microglial activation

ABSTRACT

Nod-like Receptor Protein 3 (NLRP3) inflammasome activation is known to lead to microglia-mediated neuroinflammation. Methamphetamine is known to induce microglial activation. However, whether NLRP3 inflammasome activation contributes to the microglial activation induced by methamphetamine remains elusive. P53-up-regulated modulator of apoptosis (PUMA) is a known apoptosis inducer; however, their role in microglial activation remains poorly understood. Methamphetamine treatment induced NLRP3 inflammasome activation as well microglial activation in animal model. Intriguingly, downregulation of PUMA significantly inhibited the activation of microglia. Methamphetamine treatment increased the expression of PUMA at protein level but not mRNA level. Further study indicated that PUMA expression was regulated at post-transcriptional level by miR-143, which was decreased in methamphetamine-treated cells via the negative transcription factor nuclear factor-kappa B1 (NF-κB1). Using gain- and loss-of-function approaches, we identified a unique role of miR-143/PUMA in mediating microglial activation via regulation of NLRP3 inflammasome activation. These findings provide new insight regarding the specific contributions of the miR-143/PUMA pathway to NLRP3 inflammasome activation in the context of drug abuse.

1. Introduction

Methamphetamine abuse is a major social and health concern. Methamphetamine is a popular addictive pharmacological psychostimulant of the central nervous system (CNS), and its use is associated with multiple adverse neuropsychiatric reactions as well as neurotoxicity to the dopaminergic and serotonergic systems of the brain (Kaushal and Matsumoto, 2011; Northrop et al., 2016; Yu et al., 2015). Microglia, which are CNS cells of myeloid lineage, play an important role in immune surveillance and are known to be actively involved in various neurologic pathologies (Colonna and Butovsky, 2017; Mrdjen et al., 2018). Methamphetamine-induced neurotoxicity is associated with microglial activation that is thought to participate in either pro-toxic or protective mechanisms in the brain. Imaging studies have demonstrated that methamphetamine addicts exhibit prominent microglial activation in regions of dopaminergic and serotoninergic innervation (Sekine et al., 2008).

Nod-like Receptor Protein 3 (NLRP3) inflammasome activation is known to lead to microglia-mediated neuroinflammation and dopaminergic neuronal degeneration (Zhou et al., 2016). Microglia express the NLRP3 inflammasome and secrete interleukin-1β (IL-1β) in an NLRP3 inflammasome-dependent manner. Activation of the NLRP3 inflammasome causes the maturation and release of several proinflammatory cytokines, such as IL-1β and IL-18, so it plays a critical role in the initiation of inflammation and the development of the immune response (Scheiblich et al., 2017). The NLRP3 inflammasome is a cytosolic protein complex composed of NLRP3, ADC, and caspase-1 and is assembled in response to both microbial infection and endogenous "danger signals". Although methamphetamine is known to induce microglial activation, the mechanism of NLRP3 inflammasome activation contributes to the microglial activation induced by methamphetamine remains unclear.

P53-up-regulated modulator of apoptosis (PUMA) is known to be an essential apoptosis inducer. PUMA is one of the most common apoptosis inducers among the BCL2-homology 3 (BH3)-only subgroup of BCL2 family members (Akhter et al., 2014; Chipuk and Green, 2009; Thakur

* Corresponding authors at: Department of Pharmacology, School of Medicine, Southeast University, Nanjing, Jiangsu, 210009, China.
E-mail addresses: yuanzhang@seu.edu.cn (Y. Zhang), yaohh@seu.edu.cn (H. Yao).

https://doi.org/10.1016/j.toxlet.2018.10.020
Received 22 July 2018; Received in revised form 2 October 2018; Accepted 22 October 2018
Available online 28 October 2018
0378-4274/

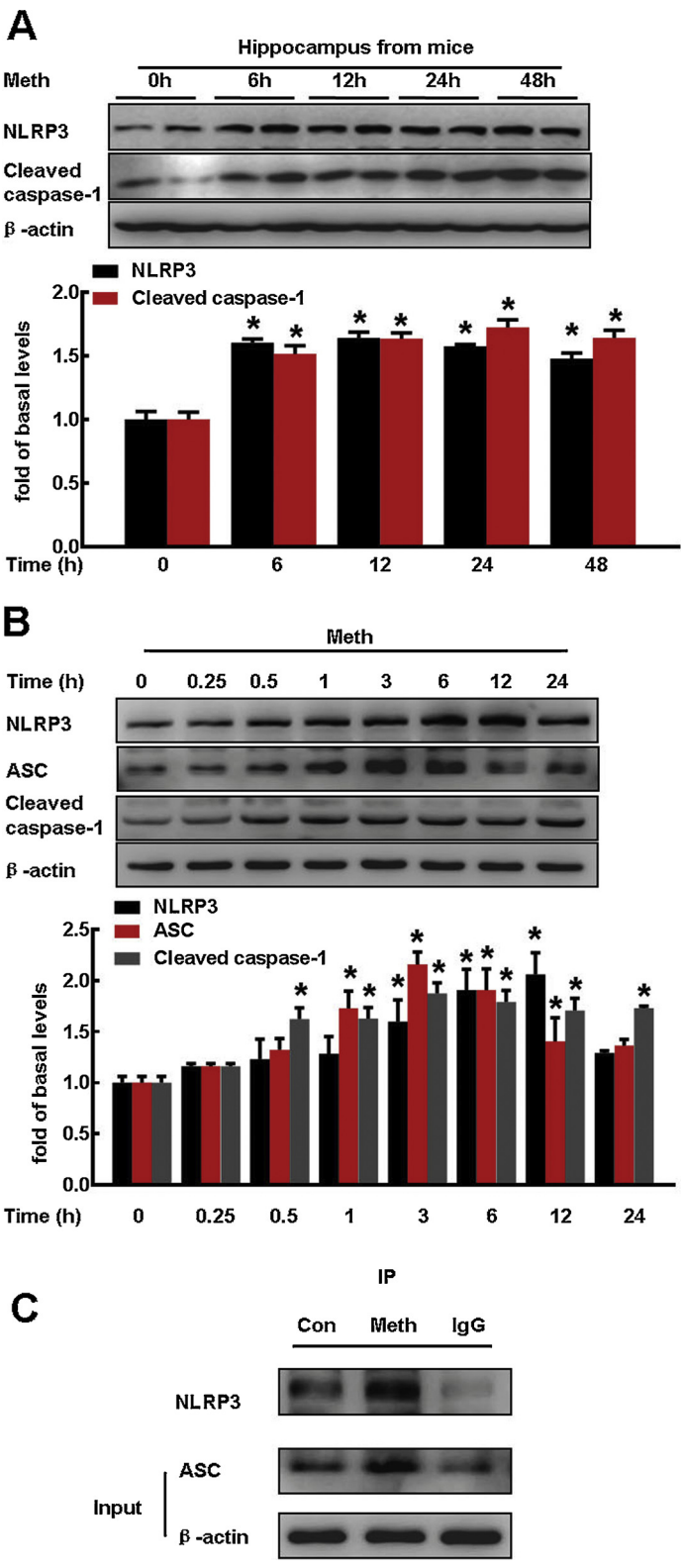

Fig. 1. Role of NLRP3 inflammasome activation in microglial activation induced by methamphetamine.
(A) The expression of the NLRP3 inflammasome and cleaved caspase-1 in the hippocampus of WT mice was determined by western blotting. The WT mice were treated with methamphetamine (i.p., 30 mg/kg) for 6, 12, 24, 48 h. N = 6 animals/group. All data were presented as mean ± SD, *p < 0.05 versus the saline-treated WT group using one-way ANOVA. Meth, methamphetamine. **(B)** Methamphetamine increased the expression of NLRP3 in BV2 cells. Cells were treated with methamphetamine (150 μM) for 0.25, 0.5, 1, 3, 6, 12, 24 h, The expression of the NLRP3 was determined by western blotting. All data were presented as mean ± SD of three independent experiments, *p < 0.05 versus the control group using one-way ANOVA. **(C)** The status of ASC binding to NLRP3 after methamphetamine treatment. Immunoprecipitation assays demonstrated that the amount of ASC in the NLRP3-immunoprecipitated protein complex decreased while the amount of total NLRP3 remained unchanged in methamphetamine-treated microglia. BV2 cells were treated with methamphetamine for 6 h, followed by immunoprecipitation. Meth, methamphetamine.

et al., 2010). In a recent study, we identified the unique role of microRNA (miR)-143/PUMA in mediating microglial survival via regulation of the interplay between apoptosis and autophagy (Zhang et al., 2016b). Although the function of PUMA in apoptosis has been extensively illustrated in various tissues, PUMA is involved in methamphetamine-induced microglial activation remains poorly understood. The NLRP3 inflammasome has been extensively investigated, however, its regulatory networks, especially mechanisms involving non-coding RNA, remain unknown. Whether miR-143/PUMA is involved in NLRP3 and microglia activation remains elusive.

Our current findings indicate that regulation of the NLRP3 inflammasome by the miR-143/PUMA axis plays a pivotal role in methamphetamine-induced microglial activation, suggesting that NLRP3 may represent a new therapeutic target to combat neuroinflammation.

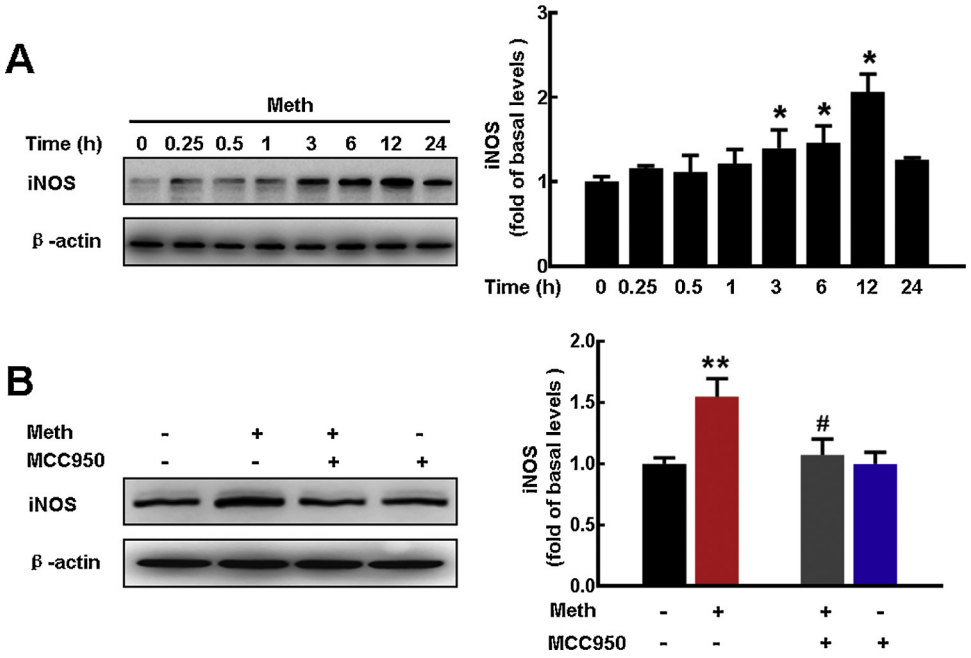

Fig. 2. Role of NLRP3 inflammasome activation in methamphetamine-induced microglial activation *in vitro*.
(A) Methamphetamine increased the expression of iNOS in BV2 cells. Cells were treated with methamphetamine (150 μM) for 0.25, 0.5, 1, 3, 6, 12, 24 h, The expression of the iNOS was determined by western blotting. All data were presented as mean ± SD of three independent experiments, *p < 0.05 versus the control group using one-way ANOVA, Meth, methamphetamine. **(B)** NLRP3 inflammasome inhibitor MCC950 significantly inhibited iNOS expression induced by methamphetamine in BV2 cells. All data were presented as mean ± SD of 3 independent experiments. **p < 0.01 versus the control without MCC950 group; #p < 0.05 versus the methamphetamine without MCC950 group using one-way ANOVA. Meth: methamphetamine.

2. Methods and materials

2.1. Reagents

Lentiviral vectors for miR-143 over expression (OE) as well as anti-miR-143 and PUMA siRNA were purchased from HANBIO (Shanghai, China). The PUMA OE plasmid (pHA-PUMA, Plasmid #16588) was obtained from Addgene (Cambridge, MA, USA). The PUMA OE lentivirus was based on the sequence of PUMA and packaged by HANBIO (Shanghai, China). Methamphetamine was ordered from the National Institute for the Control of Pharmaceutical and Biological Products (Beijing, China). The control siRNA (sc-37007) and NF-κB p50 siRNA (sc-29408) were obtained from Santa Cruz Biotechnology (Dallas, TX, USA).

2.2. Animals

Eight weeks old Adult male C57BL/6 J (wild-type) mice, weighing approximately 25.0 ± 3.0 g, were purchased from the Model Animal Research Center of Nanjing University (Nanjing, China) and after acclimatization, the mice were randomly divided into two groups (control group and methamphetamine treated group, n = 6 animals/group). All mice were randomized and housed in a temperature-controlled animal facility (24 ± 2 °C) under a 12-h/12-h light/dark cycle and fed *ad libitum*. After the animals were habituated, the mice were injected i.p. with methamphetamine (30 mg/kg) every 2 h for a total of four injections (Zhang et al., 2016a). Six, twelve, twenty-four or forty-eight hours after the last injected, the mice were euthanized and hippocampus of brain regions were dissected for further analysis of the expression of NLRP3 and cleaved caspase-1. The care and use of animals were reviewed and approved by the Institutional Animal Care and Use Committee at the Medical School of Southeast University.

2.3. Cell culture

BV2 cells, a murine immortalized microglial cell line, were obtained from the China Center for Type Culture Collection (Wuhan, China). These cells were used to characterize the effects of methamphetamine on brain microglia. The cells were routinely maintained in DMEM (10% FBS, 1% penicillin/streptomycin) and incubated at 37 °C and 5% CO_2.

2.4. Western blot analysis

Protein, including the nuclear protein fraction, was extracted in RIPA lysis buffer (Beyotime, P0013B) or using the KeyGen Nuclear and Cytoplasmic Protein Extraction Kit (KeyGen Biotech, KGP150), respectively. Then, the proteins were separated by sodium dodecyl sulfate-polyacrylamide gel electrophoresis and transferred to polyvinylidene fluoride membranes. After the membranes were blocked with 5% non-fat dry milk in Tris-buffered saline with Tween-20, they were incubated overnight at 4 °C with the following primary antibodies: anti-nuclear factor-kappa B1 (NF-κB1) (3035) and anti-Histone H3 (9715) from Cell Signaling (Danvers, MA, USA); anti-iNOS (18985-1-AP); anti-PUMA (55120-1-AP); anti-CASP1 (22915-1-AP) ; anti-ASC (10500-1-AP) and anti-NLRP3 (19771-1-AP) from Proteintech (Rosemont, IL, USA); and anti-β-actin (BS6007 M) from Bioworld (Dublin, OH, USA). The secondary antibody (horseradish peroxidase-conjugated goat anti-mouse/rabbit IgG, 1:2000) was used to detect the proteins using a MicroChemi 4.2® (DNR, Israel) digital image scanner. Band intensity was quantified using Image J software (NIH).

2.5. Real-time PCR

Total RNA was isolated from cells and subjected to reverse transcription using a PrimeScript RT Master Mix Kit (TaKaRa, RR036). Real-time PCR analysis was performed for PUMA (forward primer: 5'-ACG ACCTCAACGCGCAGTA-3'; reverse primer: 5'-CTAG TTGGGCTCCATT TCTGG-3') and β-actin (forward primer: 5'-CTAGCACCATGAAGATCA AGAT-3'; reverse primer: 5'-CCAGGATAGAGCCA CCAA-3'). Relative quantification was performed using TaKaRa SYBR® Premix Taq™ (TbI RNase H Plus) (TaKaRa, RR420). Specific primers and probes for mature miR-143 and RNU6B snRNA were obtained from RiboBio (Guangzhou, China). All reactions were run in triplicate. The amount of miR-143 was obtained through normalization to the amount of RNU6B snRNA and is reported relative to the control, as previously reported (Hu et al., 2010). The miR quantification was using the comparative Ct method ($Ct = 2^{-\Delta\Delta Ct'}$; Ct, cycle number at which the fluorescence in the reaction crosses the preset arbitrary threshold; ΔCt', difference between the Ct target and reference; ΔΔCt', difference between the ΔCt' of the test and the ΔCt' of the preassigned control)(Williamson et al., 2013).

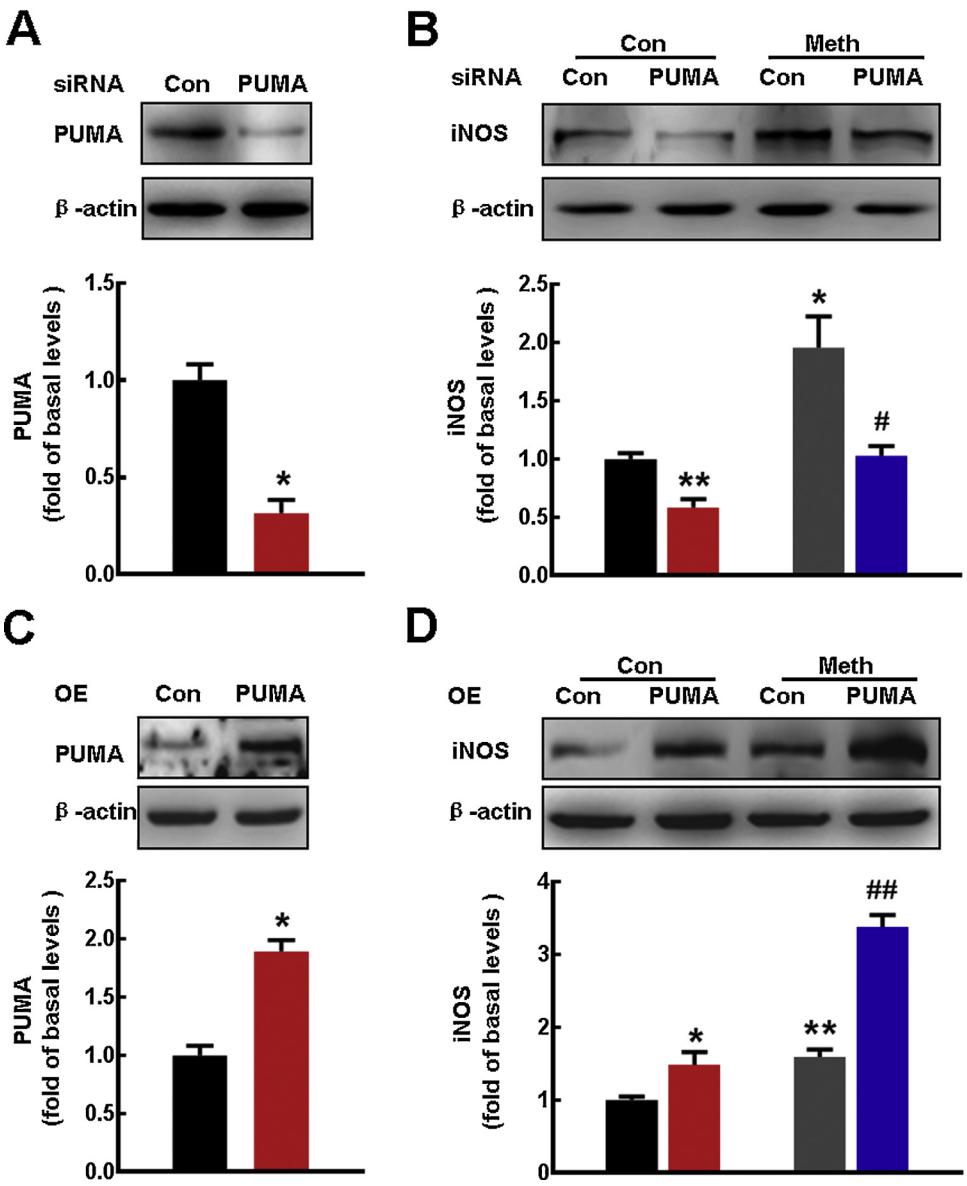

Fig. 3. Role of PUMA in the regulation of microglial activation.
(A) PUMA siRNA lentivirus successfully decreased PUMA expression. BV2 cells were transfected with PUMA siRNA lentivirus for 24 h. The expression of the PUMA was determined by western blotting. All data were presented as mean ± SD of three independent experiments, *p < 0.05 versus the control group using student's *t*-test. **(B)** Knockdown of PUMA expression by siRNA lentivirus decreased the methamphetamine-induced expression of iNOS. BV2 cells were transfected with PUMA siRNA lentivirus for 24 h, treated with methamphetamine (150 μM) for another 6 h, and then processed to determine the levels of iNOS expression using western blotting. All data were presented as mean ± SD of three independent experiments, *p < 0.05 and **p < 0.01 versus the control group; #p < 0.05 versus the control siRNA lentivirus group treated with methamphetamine using one-way ANOVA. Meth, methamphetamine. **(C)** The PUMA OE lentivirus increased PUMA expression in BV2 cells. The expression of the PUMA was determined by western blotting. All data were presented as mean ± SD of three independent experiments, *p < 0.05 versus the control group using student's *t*-test. **(D)** Transducing BV2 cells with PUMA OE lentivirus further enhanced the methamphetamine-induced increase in the expression of iNOS. BV2 cells were transfected with PUMA OE lentivirus for 24 h, treated with methamphetamine (150 μM) for another 6 h, and then processed to determine the levels of iNOS expression using western blotting. All data were presented as mean ± SD of three independent experiments, *p < 0.05 and **p < 0.01 versus the control group; ##p < 0.01 versus the control siRNA lentivirus group treated with methamphetamine using one-way ANOVA. Meth, methamphetamine.

2.6. ELISA analysis

The cell culture supernatant from BV2 cell culture after different treatments were collected to determine the levels of IL-1β using mouse IL-1β ELISA kits (R&D Systems, Inc. Minneapolis, MN) according to the manufacturer's instructions.

2.7. Chromatin immunoprecipitation (ChIP) assay

The ChIP assay was performed according to the manufacturer's instructions (Millipore, Temecula, USA). Briefly, 18.5% fresh formaldehyde was added directly to the medium for crosslinking, ensuring a final concentration of 1% formaldehyde. After 10 min incubation at room temperature, the unreacted formaldehyde was quenched with 10X glycine for 5 min at room temperature. The washed cells (cold 1X PBS, twice) were scraped with cold PBS containing 1X protease inhibitor cocktail and then centrifuged (800 g, 5 min, 4 °C) to pellet the cells. Nuclei were harvested from the cell pellet using lysis buffer containing 1X protease inhibitor cocktail. DNA was sheared by sonication. The sheared cross-linked chromatin was then diluted with dilution buffer, mixed with protein A magnetic beads and corresponding antibodies, including those for NF-κB1, histone and IgG, and then incubated overnight at 4 °C. After the mixture was washed with a series of cold wash buffers in the following order: low salt buffer, high salt buffer, LiCl buffer and TE buffer. The cross-linked protein/DNA complexes were then reversed to free DNA with elution buffer and purified using DNA purification spin columns in accordance with the manufacturer's instructions. Finally, the purified DNA was amplified via PCR to identify the promoter-region-containing NF-κB1 binding site "GGG GAGTGCCT". The sequences of the primers used to identify miR-143 bound by the transcription factor NF-κB1 were as follows: sense: 5'-CCTGGTAAAAGGGCTGTGGAA-3', anti-sense: 5'-ACCTTTGCTTCGTGG TGACT-3'.

2.8. Immunoprecipitation

To investigate the interaction between ASC with NLPR3, cells were treated with 150 μM methamphetamine and lysed with RIPA buffer. In total, 100 ml protein was incubated with 1 ml ASC antibody overnight at 4 °C and precipitated with 20 ml Protein A/G PLUS-Agarose (Santa Cruz Biotechnology, sc- 2003). After the cell pellets were rotated at 4 °C for 90 min, the cell pellets were rinsed twice with 1 ml RIPA lysis buffer and boiled for 5 min with 5XSDS loading buffer (6 ml) and RIPA lysis buffer (24 ml). Then, the protein complexes were detected using NLPR3

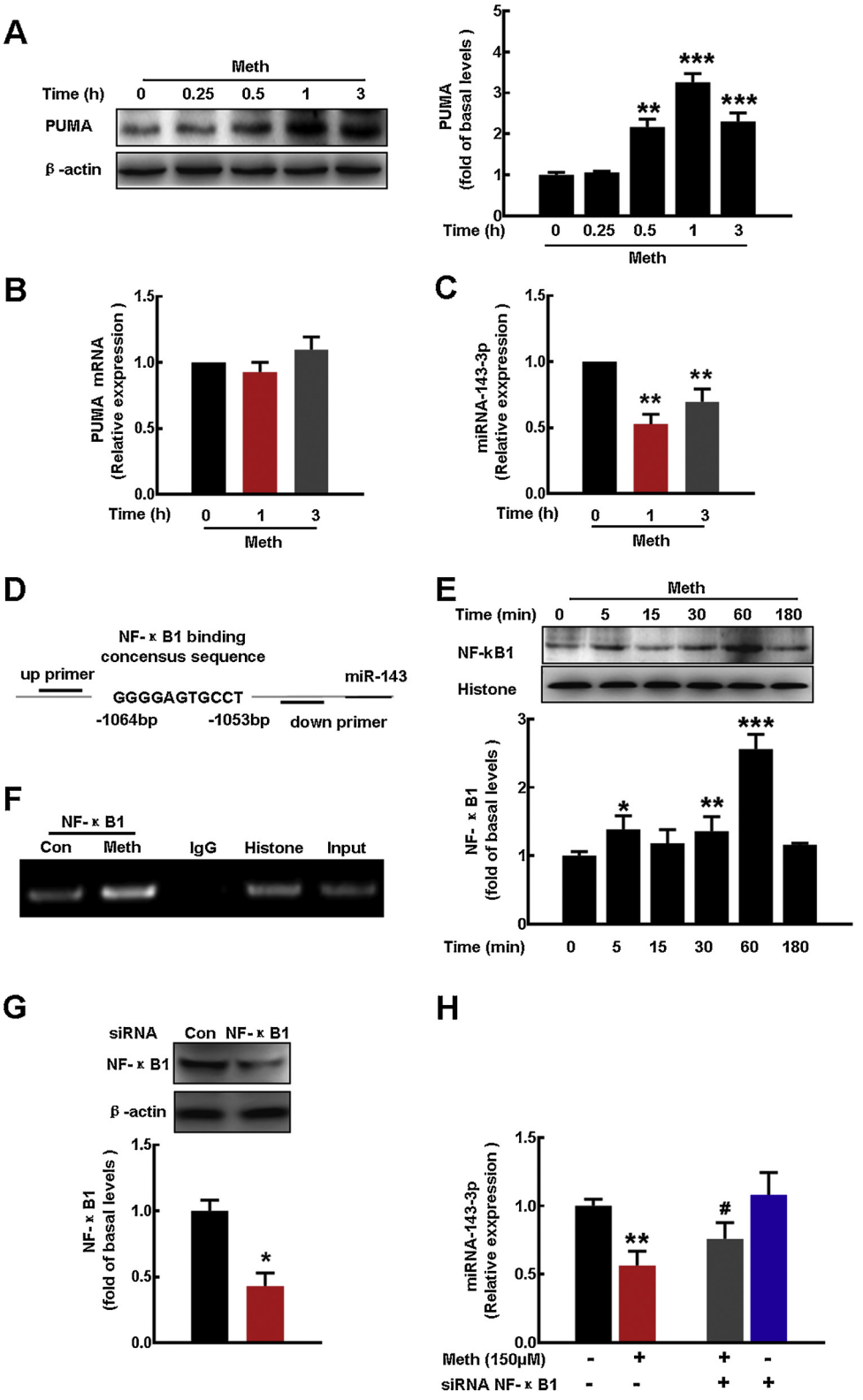

Fig. 4. miR-143 regulated PUMA expression in microglia at the post-transcriptional level. **(A)** Methamphetamine increased the protein expression of PUMA in BV2 cells. Cells were treated with methamphetamine (150 μM) for 0.25, 0.5, 1, 3 h, The expression of the PUMA was determined by western blotting. All data were presented as mean ± SD of three independent experiments, $^{**}p < 0.05$ and $^{***}p < 0.001$ versus the control group using one-way ANOVA. Meth, methamphetamine. **(B)** Methamphetamine failed to affect the mRNA level of PUMA. Cells were treated with methamphetamine (150 μM) for 1, 3 h, The expression of the PUMA at mRNA level was determined by real-time PCR. All data were presented as mean ± SD of three independent experiments, versus the control group using student's *t*-test. Meth, methamphetamine. **(C)** Methamphetamine treatment of BV2 cells significantly decreased the expression of miR-143. The expression of the miR-143 was determined by real-time PCR. All data were presented as mean ± SD of three independent experiments, $^{**}p < 0.01$ versus the control group using student's *t*-test. Meth, methamphetamine. **(D)** Illustration of the consensus binding site of NF-κB1 with the miR-143 promoter. **(E)** The methamphetamine-induced expression of NF-κB1 in the nucleus, cytoplasm and total lysates of BV2 cells. Cells were treated with methamphetamine (150 μM). All data were presented as mean ± SD of three independent experiments, $^{**}p < 0.05$, $^{**}p < 0.01$ and $^{***}p < 0.001$ versus the control group using student's *t*-test. Meth, methamphetamine. **(F)** ChIP assay demonstrating the methamphetamine-mediated binding of NF-κB1 to the miR-143 promoter. **(G)** NF-κB1 siRNA successfully decreased the expression of NF-κB1. BV2 cells were transfected with NF-κB1 siRNA for 24 h. The expression of the NF-κB1 was determined by western blotting. All data were presented as mean ± SD of three independent experiments, $^{*}p < 0.05$ versus the control group using student's *t*-test. **(H)** siRNA-mediated knockdown of NF-κB1 expression increased the methamphetamine-induced decrease in miR-143 expression. Cells were transfected with NF-κB1 siRNA for 24 h and then treated with methamphetamine (150 μM) for another 3 h; the cells were then processed to determine miR-143 expression using real-time PCR. All data are presented as the mean ± SD of three independent experiments. $^{**}p < 0.01$ versus the control group; $\#p < 0.05$ versus the control siRNA group treated with methamphetamine using one-way ANOVA. Meth: methamphetamine.

antibody; the input protein (without antibody addition) served as a control to confirm that equal amounts of total protein were used.

2.9. Statistical analyses

Statistical analysis was performed using Student's *t*-test or one-way analysis of variance (ANOVA) followed by LSD post hoc analyses (SPSS 22). The appropriate tests are indicated in the figure legends. The results were considered significant at $p < 0.05$ for ANOVA.

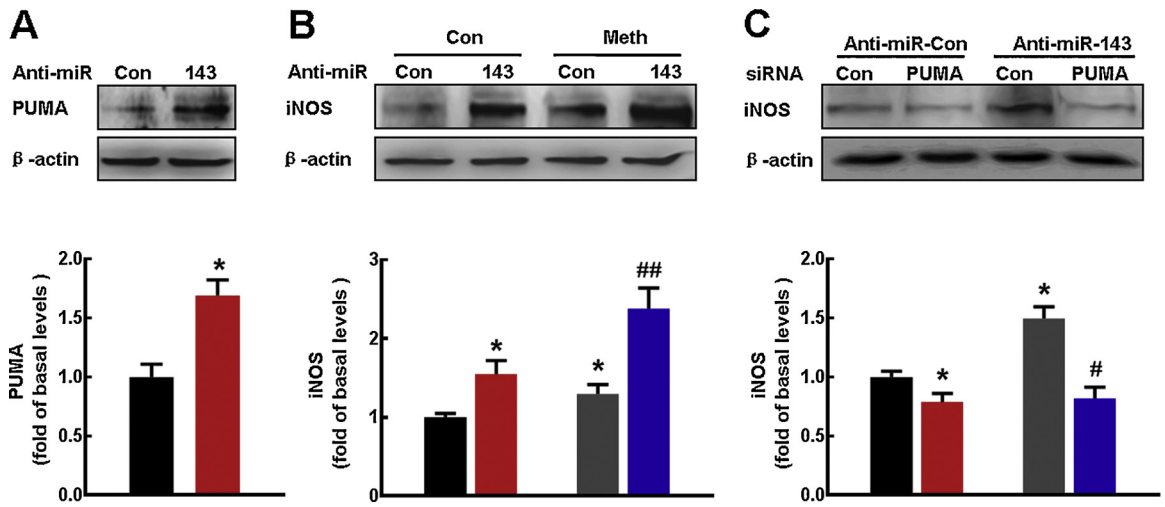

Fig. 5. Role of miR-143/PUMA in the microglial activation.
(A) Transduction of BV2 cells with anti-miR-143 lentivirus increased PUMA expression. All data are presented as the mean ± SD of three independent experiments. *p < 0.05 versus the anti-miR-control group using student's t-test. **(B)** Transducing cells with anti-miR-143 lentivirus enhanced the methamphetamine-induced increase in the expression of iNOS. Cells were transduced with anti-miR-143 lentivirus for 24 h, treated with methamphetamine (150 μM) for 6 h, and then processed to determine the expression of iNOS using western blotting. All data are presented as the mean ± SD of three independent experiments. *p < 0.05 versus the anti-miR-control group; ##p < 0.01 versus the anti-miR-control methamphetamine-treated group using one-way ANOVA. Meth: methamphetamine. **(C)** Transducing cells with the PUMA siRNA lentivirus significantly inhibited the anti-miR-143-induced increase in the levels of iNOS. Cells were co-transduced with PUMA siRNA and anti-miR-143 lentivirus for 24 h, treated with methamphetamine (150 μM) for another 6 h, and then processed to determine the expression of iNOS using western blotting. All data are presented as the mean ± SD of three independent experiments. *p < 0.05 versus the anti-miR-control co-transfected with siRNA-control group; #p < 0.05 versus the anti-miR-143 co-transfected with siRNA-control group using one-way ANOVA. Meth: methamphetamine.

3. Results

3.1. Methamphetamine induced NLRP3 inflammasome activation

To determine whether methamphetamine contributes to NLRP3 inflammasome activation. We examined the effect of methamphetamine on NLRP3 inflammasome in a methamphetamine-treated rodent model. Methamphetamine significantly increased the expression of NLRP3 as well as the cleavage of caspase-1 in the hippocampus of mice (Fig. 1A). In order to further confirm this finding *in vivo*, we further examined the effect of methamphetamine on inflammasome activation in BV2 cells. As shown in Fig. 1B, methamphetamine significantly increased the expression of NLRP3, associated speck-like protein containing a C-terminal caspase recruitment domain (ASC) and cleavage of caspase-1. Using co-immunoprecipitation assays, the amount of ASC in the NLRP3-immunoprecipitated protein complex was shown to increase while the amount of total NLRP3 remained unchanged in methamphetamine-treated BV2 cells (Fig. 1C). Taken together, these findings suggest that methamphetamine induced NLRP3 inflammasome activation.

3.2. Role of NLRP3 in the microglial activation

As an initial screen to better understand how methamphetamine affects microglial activation, we next examined the effect of methamphetamine on microglial activation. As shown in Fig. 2A, methamphetamine increased iNOS (marker for activated microglia) expression in BV2 cells with the peak time at 12 h. Pretreatment of cells with NLRP3 inflammasome inhibitor-MCC950 significantly inhibited the increased expression of iNOS induced by methamphetamine as shown in Fig. 2B. These findings suggest that NLRP3 inflammasome plays a critical role in the methamphetamine-induced microglia activation.

3.3. Role of PUMA in the regulation of microglial activation

To examine the role of PUMA in microglial activation, the expression of iNOS was examined in BV2 cells which pretreated with PUMA siRNA followed by methamphetamine treatment. As expected, PUMA siRNA decreased the expression of PUMA (Fig. 3A). Methamphetamine induced the expression of iNOS, which was significantly inhibited by PUMA siRNA (Fig. 3B). To further confirm, the effect of methamphetamine on iNOS was examined in BV2 cells transduced with a PUMA OE lentivirus. As expected, transducing BV2 cells with the PUMA OE lentivirus increased PUMA expression (Fig. 3C). In contrast to the effects of PUMA siRNA, PUMA OE enhanced the methamphetamine-induced increase in iNOS (Fig. 3D). Taken together, these findings suggest that PUMA plays a critical role in the methamphetamine-induced activation of microglia.

3.4. miR-143 regulated PUMA expression in microglia at the post-transcriptional level

Methamphetamine treatment increased PUMA protein levels (Fig. 4A), however, methamphetamine failed to affect PUMA mRNA levels (Fig. 4B). The next step was to determine whether methamphetamine mediated its effects via the induction of miR-143 and to assess the kinetics of the methamphetamine response. Methamphetamine treatment of BV2 cells significantly decreased the expression of miR-143 (Fig. 4C), which correlated inversely with PUMA expression (Fig. 4A).

Then, we sought to examine in detail the mechanisms underlying the decrease in miR-143 expression. Putative binding sites were predicted using Alggen Promo software, V3.0.2 (http://alggen.lsi.upc.es). As predicted, this analysis identified a repressor, NF-κB1, which can bind with the promoter of miRNA-143, as shown in Fig. 4D. Treating cells with methamphetamine induced the translocation of NF-κB1 into the nucleus (Fig. 4E), and methamphetamine treatment of BV2 cells increased the binding of NF-κB1 to the promoter region of miR-143, as determined by ChIP assay (Fig. 4F). Furthermore, Knockdown of NF-κB1 using siRNA significantly decreased the expression of NF-κB1 in BV2 cells (Fig. 4G). As expected, siRNA NF-κB1 inhibited the methamphetamine-induced decreased miR-143 expression (Fig. 4H). Taken together, these findings suggest that NF-κB1 acts as a repressor, negatively regulating the expression of miR-143.

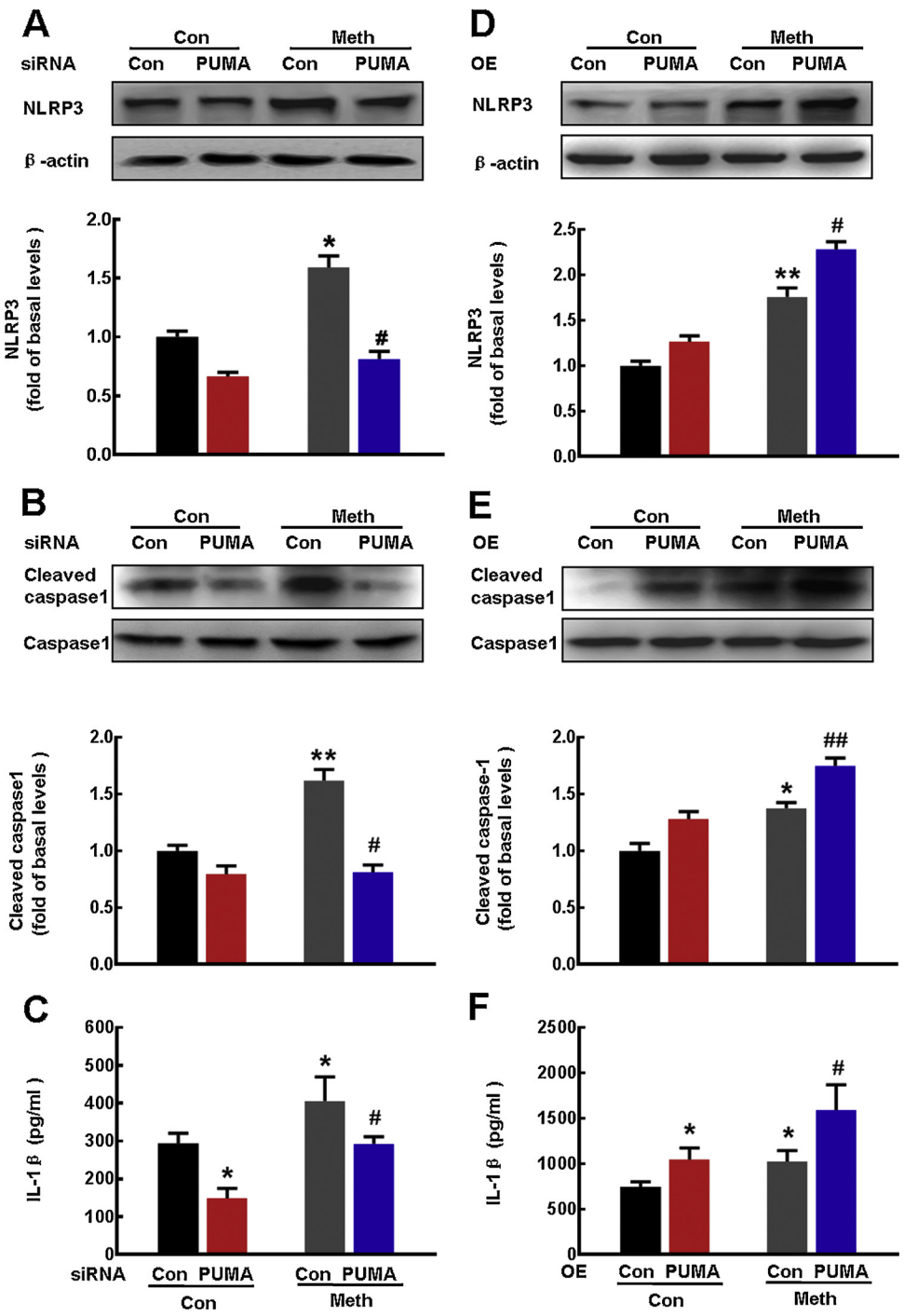

Fig. 6. Role of PUMA in methamphetamine-induced NLRP3 inflammasome activation. **(A–C)** Knockdown of PUMA expression by siRNA lentivirus decreased the methamphetamine-induced expression of NLRP3 **(A)**, cleaved caspase-1 **(B)** and IL-1β **(C)**. BV2 cells were transfected with PUMA siRNA lentivirus for 24 h, treated with methamphetamine (150 μM) for another 6 h, and then processed to determine the levels of NLRP3 and caspase-1 expression using western blotting. The supernatant was processed to determine cleaved caspase-1 expression using western blotting and IL-1β expression using ELISA. All data are presented as the mean ± SD of three independent experiments. *p < 0.05 and **p < 0.01 versus the siRNA-control group; #p < 0.05 versus the siRNA-control group treated with methamphetamine using one-way ANOVA. Meth: methamphetamine. **(D–F)** Transducing BV2 cells with PUMA OE lentivirus further enhanced the methamphetamine-induced increase in the expression of NLRP3 **(D)**, cleaved caspase-1 **(E)** and IL-1β **(F)**. BV2 cells were transduced with PUMA OE lentivirus for 24 h, treated with methamphetamine (150 μM) for another 6 h, and then processed to determine the levels of NLRP3 and caspase-1 expression using western blotting. The supernatant was processed to determine cleaved caspase-1 expression using western blotting and IL-1β expression using ELISA. All data are presented as the mean ± SD of three independent experiments. *p < 0.05 and **p < 0.01 versus the siRNA-control group; #p < 0.05 and ##p < 0.01 versus the siRNA-control group treated with methamphetamine using one-way ANOVA. Meth: methamphetamine.

3.5. Role of the miR-143/PUMA axis in methamphetamine-induced microglial activation

Having determined that miR-143 regulates PUMA expression, we then examined the role of miR-143 in microglial activation. As expected, transducing the cells with anti-miR-143 significantly increased the expression of PUMA (Fig. 5A), and further enhanced the methamphetamine-induced increase in iNOS expression (Fig. 5B). Next, to determine whether the anti-miR-143-mediated functional effects depend specifically on the up-regulation of PUMA, BV2 cells were co-transduced with lentiviral vectors expressing anti-miR-143 and PUMA siRNA. Transducing cells with the anti-miR-143 lentivirus activated microglia, and this effect was significantly inhibited in cells that were co-transduced with lentiviral vectors expressing anti-miR-143 and PUMA siRNA (Fig. 5C).

3.6. Role of PUMA in methamphetamine-induced NLRP3 inflammasome activation

Next, we examined the role of PUMA in inflammasome activation. As shown in Fig. 6A-C, methamphetamine induced the expression of NLRP3, cleaved caspase-1 and IL-1β, and these expression changes were significantly inhibited by PUMA siRNA. In contrast to the effects of PUMA siRNA, PUMA OE further enhanced the methamphetamine-induced increase in NLRP3, cleaved caspase-1 and IL-1β levels (Fig. 6D-F). Taken together, these findings suggest that PUMA plays a critical role in the methamphetamine-induced activation of the NLRP3 inflammasome.

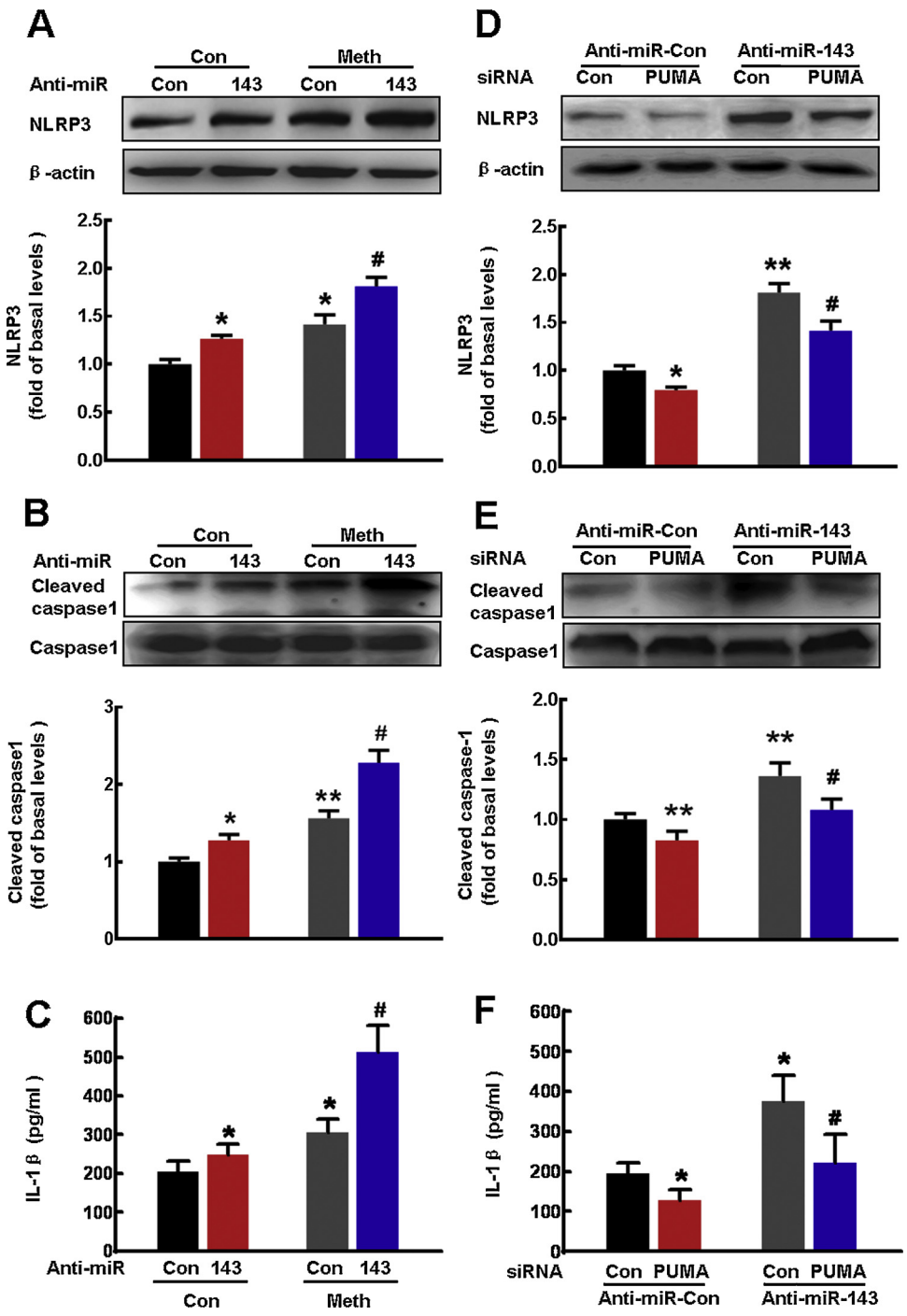

Fig. 7. Role of the miR-143/PUMA axis in methamphetamine-induced NLRP3 inflammasome activation *in vitro*. **(A–C)** Transducing cells with anti-miR-143 lentivirus enhanced the methamphetamine-induced increase in the expression of NLRP3 **(A)**, cleaved caspase-1 **(B)** and IL-1β **(C)**. Cells were transduced with anti-miR-143 lentivirus for 24 h, treated with methamphetamine (150 μM) for 6 h, and then processed to determine NLRP3 and caspase-1 expression using western blotting. The supernatant was processed to determine cleaved caspase-1 expression using western blotting and IL-1β expression using ELISA. All data are presented as the mean ± SD of three independent experiments. *p < 0.05 and **p < 0.01 versus the anti-miR-control group; #p < 0.05 and ##p < 0.01 versus the anti-miR-control methamphetamine-treated group using one-way ANOVA. Meth: methamphetamine. **(D–F)** Transducing cells with the PUMA siRNA lentivirus significantly inhibited the anti-miR-143-induced increase in the levels of NLRP3 **(D)**, cleaved caspase-1 **(E)** and IL-1β **(F)**. Cells were co-transduced with PUMA siRNA and anti-miR-143 lentivirus for 24 h, treated with methamphetamine (150 μM) for another 6 h, and then processed to determine NLRP3 and caspase-1 expression using western blotting. The supernatant was processed to determine cleaved caspase-1 expression using western blotting and IL-1β expression using ELISA. All data are presented as the mean ± SD of three independent experiments. *p < 0.05 and **p < 0.01 versus the anti-miR-control co-transfected with siRNA-control group; #p < 0.05 versus the anti-miR-143 co-transfected with siRNA-control group using one-way ANOVA. Meth: methamphetamine.

3.7. Role of the miR-143/PUMA axis in methamphetamine-induced NLRP3 inflammasome activation

Having determined that miR-143 regulated PUMA expression, we then examined the role of miR-143 in NLRP3 inflammasome activation. As shown in Fig. 7A-C, transducing the cells with the anti-miR-143 lentivirus significantly increased the expression of NLRP3, and cleaved caspase-1 as well as the level of IL-1β. Moreover, anti-miR-143 further enhanced the methamphetamine-induced increase in the expression of NLRP3, and cleaved caspase-1 as well as the level of IL-1β. Next, to determine whether the anti-miR-143-mediated functional effects depend specifically on the up-regulation of PUMA, BV2 cells were co-transduced with lentiviral vectors expressing anti-miR-143 and PUMA siRNA. Transducing cells with the anti-miR-143 lentivirus activated the NLRP3 inflammasome, and this effect was significantly inhibited in cells that were co-transduced with lentiviral vectors expressing anti-miR-143 and PUMA siRNA (Fig. 7D-F).

4. Discussion

In this study, we identified a critical role of miR-143/PUMA axis in the NLRP3 inflammasome activation induced by methamphetamine. Activation of the NLRP3 inflammasome was observed in a methamphetamine-treated rodent model. We also found that PUMA expression was up-regulated in the early stages after methamphetamine treatment. In addition, our *in vivo* and *in vitro* data provided mechanistic insight into the regulation of NLRP3 activation; we found that the miR-143/PUMA axis was involved in regulating NLRP3 inflammasome activation

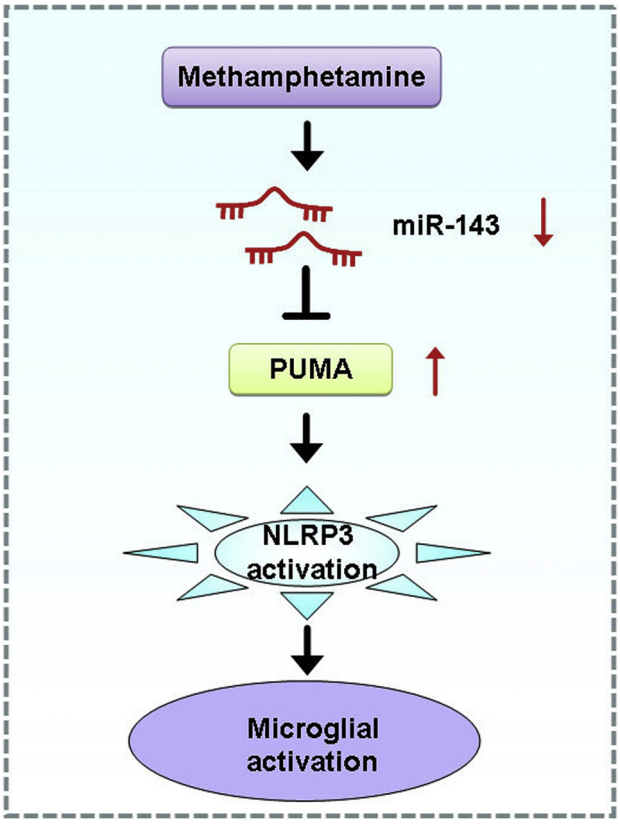

Fig. 8. Schematic diagram of miR-143/PUMA axis in NLRP3 inflammasome activation induced by methamphetamine. Methamphetamine treatment decreased the expression of miR-143, resulting upregulation of its target protein-PUMA with subsequent NLRP3 inflammasome activation and increased microglial activation.

as well as microglial activation. Targeting the NLRP3 inflammasome may be a useful therapeutic intervention for microglial activation in the context of drug abuse.

As a potent central nervous system stimulator, methamphetamine abuse can induce neuroinflammation and result in striking behavioral and cognitive changes and cardiovascular diseases, the exact mechanisms underlying methamphetamine-mediated microglial activation remained unclear. Here, we provide the first demonstration that PUMA was involved in this microglial activation, as shown by the fact that PUMA deficiency significantly inhibited microglial activation. Although PUMA is emerging as an important mediator of the deleterious effects associated with cell apoptosis (Chipuk and Green, 2009; Thakur et al., 2010), it has been shown to play a protective role in microglial survival via the induction of autophagy. In our recent study (Zhang et al., 2016b), we showed that this effect enhances microglial survival in the context of methamphetamine abuse. In this study, we observed increased PUMA expression and concomitant microglial activation after cells exposed to methamphetamine, as indicated by changes in cell morphology and the expression of iNOS (a recognized marker of microglial activation). We must note that the concentration of methamphetamine used in the *in vitro* study reported here was lower than that used in our recent study in which methamphetamine (1.5 mM) induced a bi-phasic change in PUMA expression and decreased microglial survival. Consistent with the dynamic microglial response (Kreisel et al., 2014), our study also demonstrated dynamic PUMA expression: short-term exposure to methamphetamine increased the expression of PUMA, while long-term exposure decreased its expression. These findings were further confirmed *in vitro*; a lower concentration of methamphetamine induced a sustained increased in PUMA expression, while a higher concentration of methamphetamine induced a bi-phasic change in PUMA expression-it was initially up-regulated and then decreased to the control level. It is possible that the initial methamphetamine-induced increase in PUMA expression and microglial activation played a role in the subsequent microglial decline. If so, blocking the initial microglial activation via PUMA knockdown should rescue the microglial apoptosis.

Accumulating evidence has suggested that NLRP3 inflammasome activation contributes to microglia-mediated neuroinflammation in neurodegenerative diseases such as Parkinson's disease (Zhou et al., 2016) and Alzheimer's disease (Heneka et al., 2013). Moreover, numerous studies have identified a correlation between NLRP3 and depression-like behavior (Choi and Ryter, 2014; Pan et al., 2014; Xu et al., 2016; Zhang et al., 2014); however, the NLRP3 inflammasome is involved in methamphetamine-mediated microglial activation has remained unclear. Previous studies indicated that methamphetamine treatment increased the level of IL-1β in the hypothalamus (Seminerio et al., 2012), methamphetamine potentiates Lipopolysaccharide stimulation of IL-1β production in microglia (Xu et al., 2018). However, the mechanism of NLRP3 inflammasome involved in the methamphetamine-mediated neuroinflammation remained unknown. Only one study in astrocytes demonstrated Toll-Like Receptor mediated methamphetamine-induced neuroinflammation through caspase-11 signaling pathway (Du et al., 2017). To the best of our knowledge, our results provide the upstream mechanisms of NLRP3 inflammasome involved inmethamphetamine treatment induced microglial activation.

Having determined that methamphetamine activated the NLRP3 inflammasome, we next sought to examine the upstream mechanisms responsible for regulating NLRP3 activation. Inflammasomes are multiprotein complexes that trigger the activation of caspase-1 and the maturation of IL-1β, yet the regulation of these complexes remains poorly characterized. Regarding the regulation of the NLRP3 inflammasome, previous studies have indicated that potassium influx (He et al., 2016), endoplasmic reticulum stress (Menu et al., 2012), reactive oxygen species (ROS) (Shi et al., 2016; Wu et al., 2016) and nitric oxide (Mao et al., 2013) contribute to activation of the NLRP3 inflammasome. Consistently, we also found that methamphetamine increased ROS generation in microglia (Chao et al., 2017). In addition to these known mechanisms, the *in vitro* studies we report here, which employed gain- and loss-of-function approaches involving PUMA overexpression and knockdown, demonstrated that miR-143-mediated PUMA regulation was involved in activation of the NLRP3 inflammasome. However, additional studies will be needed to unravel the mechanisms through which PUMA activates the NLRP3 inflammasome.

In our study, although methamphetamine increased PUMA expression at the protein level, we failed to detect the same effect at the mRNA level. To unravel this phenomenon, we determined that PUMA expression was regulated at the post-transcriptional level. Methamphetamine increased the expression of PUMA while concomitantly decreasing the expression of miR-143, which was negatively regulated by binding of the transcriptional repressor NF-κB1 with the promoter of miR-143. Recently, considerable evidence has implicated several factors in miRNA transcription and processing. For example, another transcription factor, CDC5, reduces miRNA promoter activity, interacts with the DCL1 complex and is required for miRNA processing in *Arabidopsis* (Zhang et al., 2013). MeCP2 inhibits gene transcription and suppresses miRNA processing by binding to the RNA-binding domains of human DGCR8 (Cheng et al., 2014). A recent study also indicated that Kaiso, a transcriptional repressor, regulates the silencing of miR-200 family by directly binding to methylated regions in the promoter (Abisoye-Ogunniyan et al., 2018). Providing further support for our study, a previous study demonstrated that androgens regulated several genes in prostate cancer cells by repressing the miR-99a/let-7c/miR-125b-2 miRNA cluster (Sun et al., 2014). Therefore, it is important to address how transcription and miRNA processing, especially of miR-143, are coordinated in the context of methamphetamine abuse.

Extending the role of miR-143 in cell proliferation (Cheng et al.,

2016; Dong and Hu, 2018), our findings suggest that transducing primary microglia with miR-143 decreased methamphetamine-induced microglial activation. Reciprocally, inhibiting miR-143 activity via anti-miR-143 further enhanced the activation of NLRP3 and microglia that occurred in the presence of methamphetamine. Notably, PUMA is not the only target gene of miR-143. Previous studies have indicated that miR-143 exerts its tumor-suppressive function by targeting oncogenes such as Syndecan-1, KRAS and C/EBPα (Ansari et al., 2016; Li et al., 2011; Sun and Zhang, 2017). Moreover, astrocyte-enriched miR-29a regulates PUMA expression and reduces neuronal vulnerability to ischemia in the forebrain (Ouyang et al., 2013). Additionally, miR-125b protects neurons against ethanol-induced apoptosis by targeting PUMA (Chen et al., 2015). Intriguingly, our study showed that the increased microglial activation induced by anti-miR-143 was abrogated by co-transduction with the PUMA siRNA lentivirus, and underscore the role of the miR-143/PUMA axis in mediating the methamphetamine-induced activation of the NLRP3 inflammasome and microglia. These findings not only extend the role of miR-143 in regulating cell survival but also add a novel molecular link between miRNA and NLRP3 inflammasome and microglial activation in the context of drug abuse.

In conclusion, our data reveal a novel role of the miR-143/PUMA axis in regulating methamphetamine-induced NLRP3 inflammasome activation. Moreover, our investigations indicate that NLRP3 inflammasome activation in microglia plays a critical role in the context of methamphetamine abuse. Altogether, our study points to regulation of NLRP3 inflammasome activation as an attractive therapeutic target for methamphetamine abusers (Fig. 8).

Financial disclosures

The authors declare no competing financial interests.

Transparency document

The Transparency document associated with this article can be found in the online version.

Acknowledgements

This work was supported by grants from the National Natural Science Foundation of China (China, No. 81473190, No. 81673410, No. 81603090 and No. 81402910). We also award for Jiangsu Specially Appointed Professor (China) and Postdoctoral Research Start Foundation of Southeast University (China, 1124000342).

References

Abisoye-Ogunniyan, A., Lin, H., Ghebremedhin, A., Salam, A.B., Karanam, B., Theodore, S., Jones-Trich, J., Davis, M., Grizzle, W., Wang, H., Yates, C., 2018. Transcriptional repressor Kaiso promotes epithelial to mesenchymal transition and metastasis in prostate cancer through direct regulation of miR-200c. Cancer Lett. 431, 1–10.

Akhter, R., Sanphui, P., Biswas, S.C., 2014. The essential role of p53-up-regulated modulator of apoptosis (Puma) and its regulation by FoxO3a transcription factor in beta-amyloid-induced neuron death. J. Biol. Chem. 289, 10812–10822.

Ansari, M.H., Irani, S., Edalat, H., Amin, R., Mohammadi Roushandeh, A., 2016. Deregulation of miR-93 and miR-143 in human esophageal cancer. Tumour Biol. 37, 3097–3103.

Chao, J., Zhang, Y., Du, L., Zhou, R., Wu, X., Shen, K., Yao, H., 2017. Molecular mechanisms underlying the involvement of the sigma-1 receptor in methamphetamine-mediated microglial polarization. Sci. Rep. 7, 11540.

Chen, X., Liu, J., Feng, W.K., Wu, X., Chen, S.Y., 2015. MiR-125b protects against ethanol-induced apoptosis in neural crest cells and mouse embryos by targeting Bak 1 and PUMA. Exp. Neurol. 271, 104–111.

Cheng, T.L., Wang, Z., Liao, Q., Zhu, Y., Zhou, W.H., Xu, W., Qiu, Z., 2014. MeCP2 suppresses nuclear microRNA processing and dendritic growth by regulating the DGCR8/Drosha complex. Dev. Cell 28, 547–560.

Cheng, W., Yan, K., Xie, L.Y., Chen, F., Yu, H.C., Huang, Y.X., Dang, C.X., 2016. MiR-143-3p controls TGF-beta1-induced cell proliferation and extracellular matrix production in airway smooth muscle via negative regulation of the nuclear factor of activated T cells 1. Mol. Immunol. 78, 133–139.

Chipuk, J.E., Green, D.R., 2009. PUMA cooperates with direct activator proteins to promote mitochondrial outer membrane permeabilization and apoptosis. Cell Cycle 8, 2692–2696.

Choi, A.J., Ryter, S.W., 2014. Inflammasomes: molecular regulation and implications for metabolic and cognitive diseases. Mol. Cells 37, 441–448.

Colonna, M., Butovsky, O., 2017. Microglia Function in the Central Nervous System During Health and Neurodegeneration. Annu. Rev. Immunol. 35, 441–468.

Dong, Y.Z., Hu, T., 2018. Effects of miR-143 overexpression on proliferation, apoptosis, EGFR and downstream signaling pathways in PC9/GR cell line. Eur. Rev. Med. Pharmacol. Sci. 22, 1709–1716.

Du, S.H., Qiao, D.F., Chen, C.X., Chen, S., Liu, C., Lin, Z., Wang, H., Xie, W.B., 2017. Toll-like receptor 4 mediates methamphetamine-induced neuroinflammation through caspase-11 signaling pathway in astrocytes. Front. Mol. Neurosci. 10, 409.

He, Y., Zeng, M.Y., Yang, D., Motro, B., Nunez, G., 2016. NEK7 is an essential mediator of NLRP3 activation downstream of potassium efflux. Nature 530, 354–357.

Heneka, M.T., Kummer, M.P., Stutz, A., Delekate, A., Schwartz, S., Vieira-Saecker, A., Griep, A., Axt, D., Remus, A., Tzeng, T.C., Gelpi, E., Halle, A., Korte, M., Latz, E., Golenbock, D.T., 2013. NLRP3 is activated in Alzheimer's disease and contributes to pathology in APP/PS1 mice. Nature 493, 674–678.

Hu, G., Zhou, R., Liu, J., Gong, A.Y., Chen, X.M., 2010. MicroRNA-98 and let-7 regulate expression of suppressor of cytokine signaling 4 in biliary epithelial cells in response to Cryptosporidium parvum infection. J. Infect. Dis. 202, 125–135.

Kaushal, N., Matsumoto, R.R., 2011. Role of sigma receptors in methamphetamine-induced neurotoxicity. Curr. Neuropharmacol. 9, 54–57.

Kreisel, T., Frank, M.G., Licht, T., Reshef, R., Ben-Menachem-Zidon, O., Baratta, M.V., Maier, S.F., Yirmiya, R., 2014. Dynamic microglial alterations underlie stress-induced depressive-like behavior and suppressed neurogenesis. Mol. Psychiatry 19, 699–709.

Li, H., Zhang, Z., Zhou, X., Wang, Z., Wang, G., Han, Z., 2011. Effects of microRNA-143 in the differentiation and proliferation of bovine intramuscular preadipocytes. Mol. Biol. Rep. 38, 4273–4280.

Mao, K., Chen, S., Chen, M., Ma, Y., Wang, Y., Huang, B., He, Z., Zeng, Y., Hu, Y., Sun, S., Li, J., Wu, X., Wang, X., Strober, W., Chen, C., Meng, G., Sun, B., 2013. Nitric oxide suppresses NLRP3 inflammasome activation and protects against LPS-induced septic shock. Cell Res. 23, 201–212.

Menu, P., Mayor, A., Zhou, R., Tardivel, A., Ichijo, H., Mori, K., Tschopp, J., 2012. ER stress activates the NLRP3 inflammasome via an UPR-independent pathway. Cell Death Dis. 3, e261.

Mrdjen, D., Pavlovic, A., Hartmann, F.J., Schreiner, B., Utz, S.G., Leung, B.P., Lelios, I., Heppner, F.L., Kipnis, J., Merkler, D., Greter, M., Becher, B., 2018. High-dimensional single-cell mapping of central nervous system immune cells reveals distinct myeloid subsets in health, aging, and disease. Immunity 48 (380–395), e386.

Northrop, N.A., Halpin, L.E., Yamamoto, B.K., 2016. Peripheral ammonia and blood brain barrier structure and function after methamphetamine. Neuropharmacology 107, 18–26.

Ouyang, Y.B., Xu, L., Lu, Y., Sun, X., Yue, S., Xiong, X.X., Giffard, R.G., 2013. Astrocyte-enriched miR-29a targets PUMA and reduces neuronal vulnerability to forebrain ischemia. Glia 61, 1784–1794.

Pan, Y., Chen, X.Y., Zhang, Q.Y., Kong, L.D., 2014. Microglial NLRP3 inflammasome activation mediates IL-1beta-related inflammation in prefrontal cortex of depressive rats. Brain Behav. Immun. 41, 90–100.

Scheiblich, H., Schlutter, A., Golenbock, D.T., Latz, E., Martinez-Martinez, P., Heneka, M.T., 2017. Activation of the NLRP3 inflammasome in microglia: the role of ceramide. J. Neurochem. 143, 534–550.

Sekine, Y., Ouchi, Y., Sugihara, G., Takei, N., Yoshikawa, E., Nakamura, K., Iwata, Y., Tsuchiya, K.J., Suda, S., Suzuki, K., Kawai, M., Takebayashi, K., Yamamoto, S., Matsuzaki, H., Ueki, T., Mori, N., Gold, M.S., Cadet, J.L., 2008. Methamphetamine causes microglial activation in the brains of human abusers. J. Neurosci. 28, 5756–5761.

Seminerio, M.J., Robson, M.J., McCurdy, C.R., Matsumoto, R.R., 2012. Sigma receptor antagonists attenuate acute methamphetamine-induced hyperthermia by a mechanism independent of IL-1beta mRNA expression in the hypothalamus. Eur. J. Pharmacol. 691, 103–109.

Shi, H., Wang, Y., Li, X., Zhan, X., Tang, M., Fina, M., Su, L., Pratt, D., Bu, C.H., Hildebrand, S., Lyon, S., Scott, L., Quan, J., Sun, Q., Russell, J., Arnett, S., Jurek, P., Chen, D., Kravchenko, V.V., Mathison, J.C., Moresco, E.M., Monson, N.L., Ulevitch, R.J., Beutler, B., 2016. NLRP3 activation and mitosis are mutually exclusive events coordinated by NEK7, a new inflammasome component. Nat. Immunol. 17, 250–258.

Sun, D., Layer, R., Mueller, A.C., Cichewicz, M.A., Negishi, M., Paschal, B.M., Dutta, A., 2014. Regulation of several androgen-induced genes through the repression of the miR-99a/let-7c/miR-125b-2 miRNA cluster in prostate cancer cells. Oncogene 33, 1448–1457.

Sun, X., Zhang, L., 2017. MicroRNA-143 suppresses oral squamous cell carcinoma cell growth, invasion and glucose metabolism through targeting hexokinase 2. Biosci. Rep. 37.

Thakur, V.S., Ruhul Amin, A.R., Paul, R.K., Gupta, K., Hastak, K., Agarwal, M.K., Jackson, M.W., Wald, D.N., Mukhtar, H., Agarwal, M.L., 2010. p53-Dependent p21-mediated growth arrest pre-empts and protects HCT116 cells from PUMA-mediated apoptosis induced by EGCG. Cancer Lett. 296, 225–232.

Williamson, B., Dooley, K.E., Zhang, Y., Back, D.J., Owen, A., 2013. Induction of influx and efflux transporters and cytochrome P450 3A4 in primary human hepatocytes by rifampin, rifabutin, and rifapentine. Antimicrob. Agents Chemother. 57, 6366–6369.

Wu, J., Li, X., Zhu, G., Zhang, Y., He, M., Zhang, J., 2016. The role of Resveratrol-induced mitophagy/autophagy in peritoneal mesothelial cells inflammatory injury via NLRP3 inflammasome activation triggered by mitochondrial ROS. Exp. Cell Res. 341, 42–53.

Xu, E., Liu, J., Liu, H., Wang, X., Xiong, H., 2018. Inflammasome Activation by Methamphetamine Potentiates Lipopolysaccharide Stimulation of IL-1beta Production in Microglia. J. Neuroimmune Pharmacol. 13, 237–253.

Xu, Y., Sheng, H., Bao, Q., Wang, Y., Lu, J., Ni, X., 2016. NLRP3 inflammasome activation mediates estrogen deficiency-induced depression- and anxiety-like behavior and hippocampal inflammation in mice. Brain Behav. Immun. 56, 175–186.

Yu, S., Zhu, L., Shen, Q., Bai, X., Di, X., 2015. Recent advances in methamphetamine neurotoxicity mechanisms and its molecular pathophysiology. Behav. Neurol. 2015, 103969.

Zhang, S., Xie, M., Ren, G., Yu, B., 2013. CDC5, a DNA binding protein, positively regulates posttranscriptional processing and/or transcription of primary microRNA transcripts. Proc. Natl. Acad. Sci. U. S. A. 110, 17588–17593.

Zhang, Y., Liu, L., Peng, Y.L., Liu, Y.Z., Wu, T.Y., Shen, X.L., Zhou, J.R., Sun, D.Y., Huang, A.J., Wang, X., Wang, Y.X., Jiang, C.L., 2014. Involvement of inflammasome activation in lipopolysaccharide-induced mice depressive-like behaviors. CNS Neurosci. Ther. 20, 119–124.

Zhang, Y., Shen, K., Bai, Y., Lv, X., Huang, R., Zhang, W., Chao, J., Nguyen, L.K., Hua, J., Gan, G., Hu, G., Yao, H., 2016a. Mir143-BBC3 cascade reduces microglial survival via interplay between apoptosis and autophagy: implications for methamphetamine-mediated neurotoxicity. Autophagy 12, 1538–1559.

Zhang, Y., Shen, K., Bai, Y., Lv, X., Huang, R.R., Zhang, W., Chao, J., Nguyen, L.K., Hua, J., Gan, G.M., Hu, G., Yao, H.H., 2016b. Mir143-BBC3 cascade reduces microglial survival via interplay between apoptosis and autophagy: implications for methamphetamine-mediated neurotoxicity. Autophagy 12, 1538–1559.

Zhou, Y., Lu, M., Du, R.H., Qiao, C., Jiang, C.Y., Zhang, K.Z., Ding, J.H., Hu, G., 2016. MicroRNA-7 targets Nod-like receptor protein 3 inflammasome to modulate neuroinflammation in the pathogenesis of Parkinson's disease. Mol. Neurodegener. 11, 28.